

Article

Variable Pressure Difference Control Method for Chilled Water System Based on the Identification of the Most Unfavorable Thermodynamic Loop

Tingting Chen * and Yuhang Han

School of Thermal Engineering, Shandong Jianzhu University, Jinan 250000, China; 17615847750@163.com

* Correspondence: chenting1208@163.com

Abstract: A variable pressure differential fuzzy control method is proposed based on the online identification method for key parameters and the fuzzy subset inference fuzzy control method of the chilled water system network model. Firstly, a phase plane fuzzy identification method is proposed for the most unfavorable thermal loop. The study focuses on analyzing the trend of room temperature deviation and deviation change in different quadrants in the phase plane. Furthermore, we establish a chilled water pipe network model that recalculates flow variation in both the main pipe and each branch pipe section to eliminate the most unfavorable thermal loop. Finally, the test platform for the fan coil variable flow air conditioning water system was designed and constructed to meet the requirements of energy-saving regulation. Additionally, the network monitoring system for the test platform was completed. The calibration and debugging results demonstrate that the monitoring error is within $\pm 5.0\%$, ensuring precise control of room temperature at the end of the branch within $\pm 0.5\text{ }^{\circ}\text{C}$. Results demonstrate that our novel method exhibits superior stability in room temperature control compared to traditional linear variable pressure differential set point controls while achieving energy saving ranging from 4.7% to 6.5%.

Keywords: variable pressure difference control; most unfavorable thermal loop; tracer direction vector angle; network model online identification



Citation: Chen, T.; Han, Y. Variable Pressure Difference Control Method for Chilled Water System Based on the Identification of the Most Unfavorable Thermodynamic Loop. *Buildings* **2024**, *14*, 1360. <https://doi.org/10.3390/buildings14051360>

Academic Editor: Gerardo Maria Mauro

Received: 22 March 2024

Revised: 29 April 2024

Accepted: 7 May 2024

Published: 10 May 2024



Copyright: © 2024 by the authors. Licensee MDPI, Basel, Switzerland. This article is an open access article distributed under the terms and conditions of the Creative Commons Attribution (CC BY) license (<https://creativecommons.org/licenses/by/4.0/>).

1. Introduction

Nowadays, the energy consumption in buildings has become a crucial issue due to its intensive usage. In developed countries, the domestic and commercial sectors can account for as high as 20% up to 40% of total energy usage [1]. The primary challenge lies in ensuring dynamic hydraulic balance within the variable water volume system (VWV system) to eliminate coupling effects between branches and effectively reduce operating energy consumption. However, if the regulation method is not reasonable, it may encourage hydraulic disorder in the pipe network, resulting in increased pump energy consumption and significant deviations from temperature set values. Therefore, achieving dynamic hydraulic balance within the VWV system's pipe network to enhance operational efficiency and accuracy of energy supply has garnered extensive attention from researchers.

In 1984, Gidwani [2] investigated optimization methods for chilled water systems such as chilled water reset, condenser water reset, chiller sequencing, chilled water storage, and variable chilled water pumping. Centrally chilled water systems offer potential energy and cost savings. In 2001, Wang [3] examined chiller units and their control strategies. The results indicated that adjusting temperature set points (i.e., employing variable temperature set point control strategy) is both easy to implement and highly efficient in terms of energy conservation. Mba et al. [4] employed ANN (Artificial Neural Network) models to predict hourly air temperature (IT) and relative humidity (IH). Accurate prediction within a building context aids in reducing air conditioning-related energy consumption. Optimal ANN structures were determined using Matlab software (R2015b) with algorithm based

on experimental data. The simulated results obtained through ANN modeling exhibited strong correlation with experimental data: coefficient of correlation was found to be 0.9850 for IT prediction and 0.9853 for IH prediction. In addition to device optimization, extensive research has been conducted by scholars on key parameter settings such as temperature, valve position, and differential pressure. With the increasing emphasis on energy-saving requirements, there has been a gradual shift from control methods with fixed set values to those with variable set values. Wang [5] proposed an adaptive online control method for chilled water systems in 2013, which improved the robustness and reliability of the control system by adjusting the water supply temperature set point and number of operating pumps. Ma [6] established a variable flow rate air conditioning system for an ultra-high-rise building in 2009, optimizing supply and return water differential pressure set points based on monitoring end valve openings and chilled water flow rate. This was achieved by adjusting pump speed to achieve optimal control process for furthest end differential pressure set points using a pipe network pressure drop model. Gao et al. [7] investigated the control process of a typical central air conditioning water system in 2011 and proposed a fault-tolerant strategy applied to a typical control method that minimized flow resistance while meeting cooling energy demand. Compared with constant differential pressure control methods, this approach resulted in significant energy-saving benefits with power consumption during start-up time being only 70% and 50% of that observed in the original system during normal operation time. Tanitsu Kazuhisa [8] introduced the minimum resistance method for regulating air conditioning chilled water flow in 1993, which involved resetting the differential pressure value based on valve position considerations through comprehensive calculation processes optimizing variable flow differential pressure setting values. Moore and Fisher [9] utilized the opening of end valves as a reference to optimize the differential pressure setting value, aiming to ensure that at least one end valve is fully open in order to achieve the lowest pump power consumption. The valve position value essentially reflects the system's response to changes in water supply demand under a certain water supply temperature, while also indicating the operating conditions of the equipment system. This approach has gained widespread recognition and become commonly used. Liu [10] establishes an analytical model for a parallel chilled water pump set with particular emphasis on the crucial role of the adjustment characteristic of the bypass loop. Operational characteristics of a pump set comprising four identical pumps are thoroughly investigated under five different control strategies. It is suggested that a hybrid control strategy, combining single pump variable frequency with power frequency pump quantity control, proves most suitable for achieving variable flow in chilled water systems characterized by low flow ratios or high supply–return water differential pressures. The potential running programs of primary–secondary–tertiary variable flow pumps were analyzed in accordance with the characteristics of the current three-level variable flow pumps [11]. The total energy consumption of the chilled variable flow pumps in cooling season was compared with that of the conventional secondary pump system. Illustrated by a case of example, 30.61% of energy saving was obtained with the three-level variable flow pumps. Based on the above conclusions, Zhao Tianyi [12] put forward the concept of the most unfavorable thermal loop of the air conditioning water system with the VAV air conditioning units as the main installations. The most unfavorable thermal loop is used as a reference basis for control, and the Mamdani type variable differential pressure set point fuzzy control method for air conditioning system is proposed. The effectiveness and energy-saving effect of the method on the all-air variable air volume air conditioning water system are verified through experimental studies. The method is based on valve position feedback, which also inherits the limitation of restricted scope of application in valve position control. The system needs to satisfy that the valve position feedback exists, and its value is accurate. I N Suamir [13] simulated and optimized chilled water circuit system of a central air conditioning plant applied for a five-star hotel. Thermodynamic analyses and numerical simulations were established to evaluate chilled water flow rate. Optimization on the chilled water flow rate between primary and secondary circuits by

implementing a variable speed pumping system incorporated with a balancing valve was estimated to potentially improve temperature performance and economic viability of the chiller plant operation. To sum up, from the proposal of the most unfavorable thermal loop to the practical application process, many previous works have been conducted; however, the current research is mainly focused on the air conditioning control system based on the continuous valve position feedback. The most unfavorable thermal loop exists in different forms of air-conditioned water systems. The differential pressure optimal reset process selected in the reference basis should be able to reflect different forms of air conditioning water system end-user load demand, so as to achieve the purpose of the air conditioning system to deliver energy, which has more practical significance in the study of energy-saving operation and control of air conditioning water system.

Modeling of chilled water systems is mainly concerned with the study of resistance models and their applications. It is well known that the water system pipe network model consists of the equations of each node and loop, including nonlinear equations, which are difficult to solve directly. In 1936, Hardy-Cross [14] proposed an iterative computation method for nonlinear systems of equations, and over the past eighty years, the theory and methodology of pipe network design have been rapidly developed. Graph theory and mathematical programming languages have gradually become the main tools for pipe network analysis, and the nodes (or pipe segments) on the pipe network are calculated and analyzed. The results are more accurate, and the calculation accuracy meets the actual needs. In 2021, Junqi Yu [15] proposed a distributed iterative optimization algorithm based on the novel distributed control architecture and the alternating direction method of multipliers (ADMMs) with regular term. Compared with one strategy that is not optimized, the operation strategy optimized by the proposed algorithm can save energy about 28.54% while realizing the dynamic hydraulic balance of the pipe network. L. Morales [16] demonstrated the utilization of LAMDA (multivariable data analysis learning algorithm) in the advanced control of building HVAC systems. A new inference method integrated into LAMDA was employed to calculate control actions that drive the system to a zero-error state. The proposed LAMDA control effectively mitigated interference by suggesting non-emergent control actions and outperformed other comparative methods. Cai [17] developed the MODI approach for structured planning processes of pattern-based control algorithms in building energy systems, introduced a documented method for reporting pattern-based control algorithms in Industrial Base Classes (IFCs), facilitated data sharing between BLMS, and presented a software-assisted approach to automatically generate PLC code for implementing these algorithms. The results demonstrate that the schema-based control strategy can be automatically implemented in the PLC program based on IFC data.

In summary, despite considerable efforts by scholars in the field of variable pressure differential control for variable flow systems, significant progress has been achieved, as shown in Table 1. However, a more comprehensive approach remains elusive. In this paper, a novel method was proposed, which solved the problem of re-normalization of pressure difference set points. The problem is decoupled into two sub-problems in this paper. Firstly, in terms of identifying the energy balance of each end branch, the identification method of the most unfavorable thermal loop was proposed. Secondly, the flow distribution characteristics of the pipe network were considered with the most unfavorable thermal loops appearing at different locations, and the experimental verification analysis was carried out.

Table 1. Summary table of primary partial citations.

Year	Authors	The Literature Review	Key Results Related to Work Outcomes
1984	Gidwani, B.N [2]	Investigated optimization methods for chilled water systems such as chilled water reset, condenser water reset, chiller sequencing, chilled water storage, and variable chilled water pumping.	Centrally chilled water systems offer potential energy and cost savings.
2013	Wang, N., J. Zhang, and X. Xia [5]	An adaptive online control method for chilled water systems was proposed.	It improved the robustness and reliability of the control system by adjusting the water supply temperature set point and number of operating pumps.
2009	Ma, Z. and S. Wang [6]	A variable flow rate air conditioning system for an ultra-high-rise building was established.	This was achieved by adjusting pump speed to achieve optimal control process for furthest end differential pressure set points using a pipe network pressure drop model.
2003	Moore and Fisher [9]	Utilized the opening of end valves as a reference to optimize the differential pressure setting value, aiming to ensure that at least one end valve is fully open in order to achieve the lowest pump power consumption.	The valve position value essentially reflects the system's response to changes in water supply demand under a certain water supply temperature, while also indicating the operating conditions of the equipment system.
2015	Xuefeng, L. [10]	An analytical model for a parallel chilled water pump set was established, with particular emphasis on the crucial role of the adjustment characteristic of the bypass loop.	A hybrid control strategy proves most suitable for achieving variable flow in chilled water systems characterized by low flow ratios or high supply–return water differential pressures.
2016	Tianyi Zhao [12]	The most unfavorable thermal loop is used as a reference basis for control, and the Mamdani type variable differential pressure set point fuzzy control method for air conditioning system is proposed.	The effectiveness and energy-saving effect of the method are verified through experimental studies.
2020	Suamir, I.N. [13]	Chilled water circuit system of a central air conditioning plant was applied to a five-star hotel. Thermodynamic analyses and numerical simulations were established to evaluate chilled water flow rate.	Optimization on the chilled water flow rate between primary and secondary circuits by implementing variable speed pumping system incorporated with a balancing valve was estimated to potentially improve temperature performance and economic viability of the chiller plant operation.
1936	Hardy-Cross [14]	An iterative computation method for nonlinear systems of equations was proposed.	The results are more accurate, and the calculation accuracy meets the actual needs.
2020	L. Morales [16]	Demonstrates the utilization of LAMDA (multivariable data analysis learning algorithm) in the advanced control of building HVAC systems.	A new inference method integrated into LAMDA is employed to calculate control actions that drive the system to a zero-error state.

2. Problem Descriptions

The optimization problem of achieving dynamic hydraulic balance in the chilled water pipe network of the central air conditioning system aims to distribute flow among various branches with minimum energy consumption by adjusting the state of end branch valves and frequency of circulating pumps, based on predicted flow demands obtained from end-load prediction results. In this study, we decompose this optimization problem into two sub-problems: (I) determining changes in flow demand for each branch based on differences between measured and set values of end space temperature; (II) optimizing pump flow and head to achieve optimal operation with lowest energy consumption, considering system's differential pressure and total flow demand. As shown in Figure 1, the chilled water system pipe network model is established.

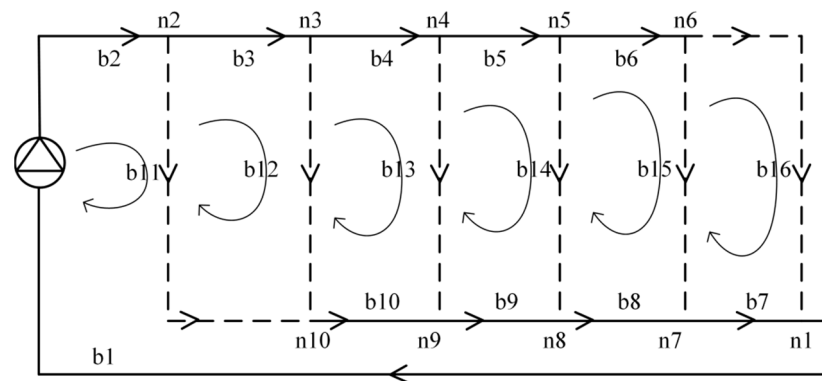


Figure 1. Directional schematic diagram of the pipe network model of the test system.

As shown in Figure 1, the solid line is the water supply pipe, and the dashed line is the return water pipe. The arrow represents the direction of water flow. $b_1 \sim b_{16}$ refers to the pipelines numbered 1~16, in which $b_1 \sim b_{10}$ is the main main pipe, $b_{11} \sim b_{16}$ is the branch pipe, the pressure drop of pipeline b_i is DP_i , the flow rate is Q_i , and the impedance is S_i . $n_1 \sim n_{16}$ are nodes 1 to 16. The model has a total of six circulating waterways with one FCU in each branch.

Description of problem 1:

To address the issue of flow demand for each branch, it is essential to obtain/forecast based on the end-load prediction results. As shown in Figure 2, the response process of the controlled system in the phase plane exhibits a trajectory curve from the initial state A (starting point) to the target state O (desired state), where $S(kT)$ represents the system's state at a given time ($e(kT)$, $ec(kT)$). I II III and IV is four different quadrants. The blue lines $e = 0$ and $ec = 0$. The phase plane method provides an intuitive depiction of dynamic response trajectory characteristics in control systems, and adjusting deviation, deviation change, and control quantity according to these characteristics can enhance control system performance.

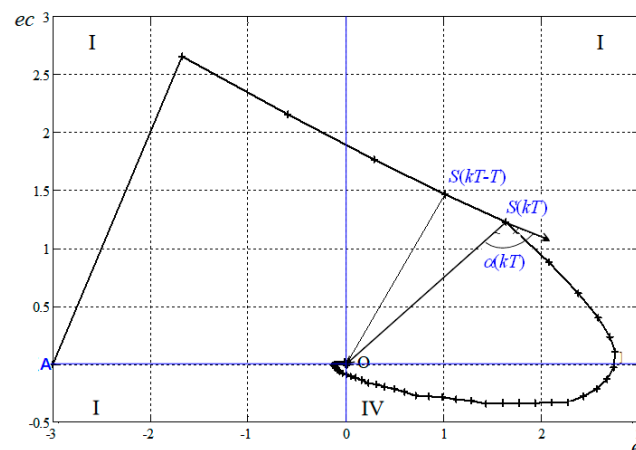


Figure 2. Control system phase plane coordinate system and system response trajectory.

For each end branch of the air conditioning water system, if the indoor temperature and its set value of $e_i = 0$ and $ec_i = 0$ at a certain time, it is obvious that the heat supply and demand of the air conditioning room are in a state of balance at this time. It can be pre-eminently seen that for the end branch i , if its end $O_i(0,0)$ is taken as the reference point, the relative positions of each point on the phase plane and O_i point reflect the degree of heat supply and demand balance of the end branch i . Obviously, the closer the state point $S_i(kT)$ on the phase plane of a certain end branch of the water system is to the O_i point, the smaller the heat supply and demand imbalance of the end branch i . Conversely, the

farther the state point S_i (kT) of the water system is from the O_i point, the greater the heat supply and demand imbalance of the end branch. For all the end branches of the water system, the one with the largest imbalance between heat supply and demand is the most unfavorable thermal loop. In addition, in Figure 2, if S_i (kT - T) is taken as the starting point and S_i (kT) as the ending point, it can be defined as the i end branch control state tracer vector, which can also be called the root trajectory vector, which can be called the root trajectory target vector, and the angle formed with the real-time feature vector is called the α_i (kT). The analysis shows that when α_i (kT) $> 90^\circ$, the system operating state point S_i (kT) will deviate more and more from the target point O , and the control intensity should be increased. When α_i (kT) $< 90^\circ$, the system motion state response S_i (kT) will be more and more biased to the target point O ; at this time, the original control intensity can be kept unchanged, but also can be appropriately increased. When α_i (kT) $= 90^\circ$, that is, the system operating state response S (kT) will move in a circle around the target point O , and the control intensity should be increased.

Description of problem 2:

The determination of the number and location of the most unfavorable thermal circuits, as well as the degree of heat supply and demand imbalance, provides crucial reference information for energy conservation control in air conditioning water systems. However, due to the impact of different resistance characteristics on flow distribution within each branch during heat/cold supply by the system, establishing a pipe network model for the air conditioning water system and predicting real-time flow distribution characteristics within this network using an identification model before variable flow regulation can significantly contribute to achieving energy saving and enabling frequency conversion control of pump variable pressure difference setting based on the most unfavorable thermal loop.

Theoretical analysis and experimental research enable the exploration of various valve structures, as well as the relationship between flow, pressure difference, valve design, selection, and practical control. However, in real-world systems, due to installation limitations, the dynamic relationship between valve opening, resistance before and after the valve, and flow rate often deviates significantly from test conditions. Therefore, it is necessary to further refine the dynamic adjustment model for these variables during actual flow rate adjustments. This provides a foundational model for variable flow control in system applications. Furthermore, an analysis of progress made in simulating air conditioning water system pipe network models reveals extensive research on dynamic mathematical models such as fan coils, pipe networks valves, and pumps for energy-saving regulation and control purposes. These models play a crucial role in optimizing energy-saving methods. However, their application in practical control engineering remains limited.

3. Methodology

3.1. Characterization of the Response Trajectory of the Most Unfavorable Thermal Loop in the Phase Plane

In order to represent the room temperature of the i th end branch in the water system on the phase plane at the moment of kT, let S_i (e_i (kT), ec_i (kT)) be the current moment room temperature state and S_i (e_i (kT - T), ec_i (kT - T)) be the previous moment room temperature state. α_i (kT) is the real-time tracer vector of the phase plane root trajectory of the room temperature of the air conditioning room of the i branch, which reflects the current position and change direction of the room temperature.

According to the definition of deviation, it is easy to obtain the following:

$$ec_i(kT) = e_i(kT) - e_i(kT - T) \quad (1)$$

that is, in the phase plane, when the room temperature state S_i (kT - T) at the previous moment is known, it is known according to Equation (1) that the room temperature state point S_i (e_i (kT), ec_i (kT)) at the current moment will be distributed on line L: ec_i (kT) = e_i

After the above analysis, it can be seen that in the known $S_i(kT - T)$, its state point $S_i(kT)$ at the moment of kT will have an infinite number of possible locations, and the $S_i(kT)$ and end point O distance size reflects the end of the water system branch i of the thermal energy supply and demand imbalance degree. This undoubtedly finds a judgment basis for further using the phase plane to determine the most unfavorable thermal loop.

To specifically calculate the relative distance between point $S_i(kT)$ and point O , a vertical line is made through point O . The intersection of this vertical line with l , M , is the closest point to point O on line l . If $S_i(kT)$ coincides with point M , then the imbalance between heat supply and demand $\Phi_i(\tau)$ is minimum, and the further point $S_i(kT)$ is from M , the larger $\Phi_i(\tau)$ is. Since the value range of e_i is $(-\infty, +\infty)$, the relative distance between point $S_i(kT)$ and point M also varies within $(-\infty, +\infty)$, i.e., it is difficult to judge the relative position distance relationship between the above two points in the phase plane within such a large variation range; for this reason, the concept of real-time tracer direction vector angle is introduced below.

The direction vector of straight line $L = (1,1)$.

Real-time tracer vectors are $(e_i(kT) - e_i(kT - T), ec_i(kT) - ec_i(kT - T))$,

$\beta_i(kT)$ is defined as the real-time tracer direction vector angle, i.e., the vector with the real-time tracer vector of the vector, and is calculated as follows:

$$\beta_i(kT) = \arccos\left(\frac{S_i(kT)S_i(kT - T) \cdot \vec{d}}{\left|S_i(kT)S_i(kT - T)\right| \cdot \left|\vec{d}\right|}\right) \quad (2)$$

Obviously, the variation range of $\beta_i(kT)$ on the graph is $(0,180)$, so the above judgment of the most unfavorable thermal loop within the value range of $(-\infty, +\infty)$ between point S_i and point M is transformed into the judgment of the most unfavorable thermal loop within the value range of $(0,180)$ of β_i , and the difficulty of judgment is greatly reduced.

In particular, when point S_i coincides with point M , the real-time tracer direction vector angle is

$$\gamma_i(kT) = \arccos\left(\frac{MS_i(kT - T) \cdot \vec{d}}{\left|MS_i(kT - T)\right| \cdot \left|\vec{d}\right|}\right) \quad (3)$$

$\beta_i(kT)$ and point $S_i(kT)$ are one-to-one correspondence. The larger $\beta_i(kT)$ is, the larger $e_i(kT)$ is, and the more likely $S_i(kT)$ is distributed in quadrant I. When the system state point $S_i(kT)$ coincides with point M , $\beta_i(kT) = \gamma_i(kT)$, the system state point $S_i(kT)$ has the fastest tendency to approach target point O . The farther it is from point M , the farther it is from target point O . The larger the value of $\Phi_i(\tau)$, the greater the possibility of this branch becoming the most unfavorable thermal loop. From Figure 3 and Equation (2), the end of the air conditioning water system branches of the heat supply imbalance and the possibility of the most unfavorable thermal loop in the phase plane can be analyzed.

1. Fuzzy recognition variables and their fuzzy levels

According to the above analysis, the appearance of the most unfavorable thermal loop of the air conditioning water system at a certain moment can be determined by $e_i(kT)$ and $\beta_i(kT)$. Obviously, the relationship between the possibility of the appearance of the most unfavorable thermal loop and $e_i(kT)$ and $\beta_i(kT)$ is expressed by an accurate mathematical model; for this reason, the fuzzy identification method is adopted here to solve the problem.

From the defining equation of the tracer direction vector entrainment angle β_i , it is clear that when it is a zero vector, this angle does not exist, and the most unfavorable thermal loop degree cannot be identified by the magnitude of $\beta_i(kT)$. Therefore, the identification process includes two working conditions.

$$\text{Case 1: } S_i(kT)S_i(kT - T) = \vec{0}$$

At this point, point $S_i(kT - T)$ coincides with point S_i , $ec_i(kT) = 0$, i.e., point $S_i(kT - T)$ and point $S_i(kT)$ are on the e axis. $e_i(kT)$ can be identified by the magnitude of $e(kT)$ at this point. $e_i(kT)$ is identified in the range $(-1.5, +1.5)$; therefore, the corresponding theoretical domains of the fuzzy levels NB to PB of $e_i(kT)$ are $\{(-\infty, -1.0), (-1.5, -0.5), (-1.0, 0), (-0.5, 0.5), (0, 1.0), (0.5, 1.5), (1.0, +\infty)\}$.

Case 2: $S_i(kT)S_i(kT - T) \neq 0$

At this time, the tracer direction vector angle $\beta_i(kT)$ exists, $\beta_i(kT)$ and $e_i(kT)$ will jointly determine the fuzzy level of the end branch thermal energy supply and demand imbalance degree, and the range of $\beta_i(kT)$ is 0° to 180° . To this end, the theoretical domain $(0^\circ - 180^\circ)$ of $\beta_i(kT)$ can be divided into seven fuzzy subsets $i(kT)$ with the following domains: $\{(-\infty, -1.0), (-1.5, -0.5), (-1.0, 0), (-0.5, 0.5), (0, 1.0), (0.5, 1.5), (1.0, +\infty)\}$.

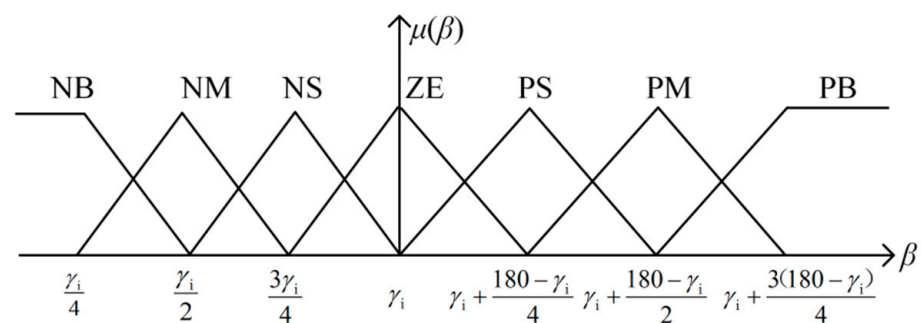
According to the range of variation in the imbalance between heat energy supply and demand (i), its thesis domain is

$[(-\infty, -0.2), (-0.3, -0.1), (-0.2, 0), (-0.1, 0.1), (0, 0.2), (0.1, 0.3), (0.2, +\infty)]$.

For the convenience of reasoning, $e_i(kT)$, $\beta_i(kT)$, and (i) are divided into 7 fuzzy classes, namely {NB, NM, NS, ZE, PS, PM, PB}. For the above 7 fuzzy levels of thermal energy supply and demand imbalance $\Phi_i(\tau)$, their physical meanings are as follows: ZE level is the area with the smallest $\Phi_i(\tau)$. If the recognition result is ZE, it means that the thermal energy supply and demand imbalance of the branch is close to or even 0 at the current moment. The loop does not belong to the most unfavorable loop. If the recognition result is PS, PM, or PB, it means the loop does not belong to the most unfavorable loop. The PB level indicates that it is most likely to belong to the most unfavorable thermal loop. If the identification result is NS, NM, or NB, it means that the heat supply of the branch is excessive at the current moment. The reverse regulation is needed. Comparing the identification results of the fuzzy level of the imbalance between the heat supply and demand of each branch $\Phi_i(\tau)$, the branch with the highest fuzzy level is the most unfavorable thermal loop in the system at the current moment.

2. Affiliation function of fuzzy variables

The affiliation functions of fuzzy variables are triangular, body-shaped, and Gaussian. The study shows that the shape of the affiliation function has little influence on the control effect of fuzzy identification, and the greater influence on the identification effect is the size of the maximum affiliation degree of the intersection of adjacent fuzzy subsets, which determines the affiliation function of each characteristic index. The characteristics of the affiliation function have little influence on the control effect of fuzzy recognition, and what has greater influence on the recognition effect is the size of the maximum affiliation of the intersection of adjacent fuzzy subsets, that is, the size of its inner product. The choice of the triangular affiliation function is sufficient to make the model robust and of high enough resolution, as shown in Figure 4.



(a) The affiliation function of β_i

Figure 4. Cont.

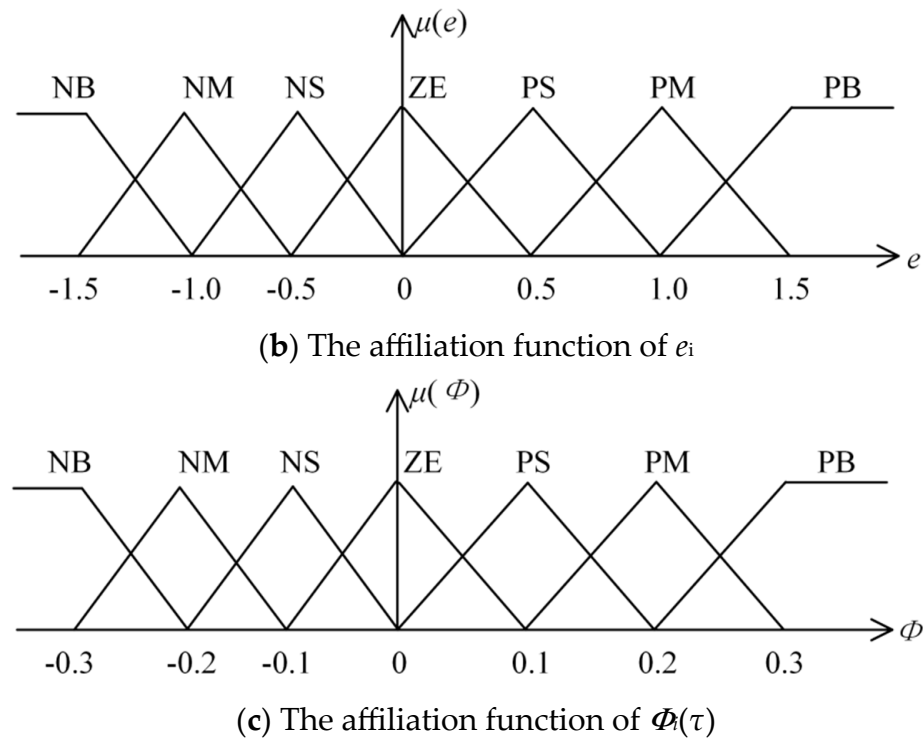


Figure 4. Phase plane eigenvector membership function.

According to the above variable characteristics in this paper, the Mamdani fuzzy model (model form, variable fuzzy domain, affiliation function) of the role fuzzy subset inference method is used here. The M model is a two-input, single-output model structure, and for the input quantities a and b, M model output c can be expressed as $c = M(a, b)$. The M model of an end branch i with dual input β_i (kT) and e_i (kT) and single output i (kT) fuzzy rules of the following form:

If β_i (kT) is A_j and e_i (kT) is B_k , then Φ_i (kT) is C_{jk} ($j, k = 1, 2, \dots, 7$)

Where j,k denotes 7 fuzzy levels {NB, NM, NS, ZE, PS, PM, PB}, β_i (kT) is the real-time tracer direction vector angle, e_i (kT) is the deviation of the room temperature measurement from its set value, $\Phi_i(\tau)$ is the thermal energy supply and demand imbalance, A_j is the fuzzy subset of the room temperature deviation, B_k is the fuzzy subset of the real-time tracer direction vector angle, and C_{jk} is the fuzzy subset of the thermal energy supply and demand imbalance.

Based on the above analysis of the characteristics of the most unfavorable thermal loop in the phase plane diagram, the following fuzzy rule table is established, as shown in Table 2.

Table 2. Fuzzy identification rules for refrigeration conditions.

β_i (kT) \ e_i (kT)	e_i (kT)						
	NB	NM	NS	ZE	PS	PM	PB
NB	NB	NB	NB	NB	NM	NS	ZE
NM	NB	NB	NB	NM	NS	ZE	PS
NS	NB	NB	NM	NS	ZE	PS	PM
ZE	NB	N	NS	ZE	PS	PM	PB
PS	NM	NS	ZE	PS	PM	PB	PB
PM	NS	ZE	PS	PM	PB	PB	PB
PB	ZE	PS	PM	PB	PB	PB	PB

Considering the characteristics of the action fuzzy subset inference method, such as fast inference and simple calculation process, and the requirement of online identification of this system, the action fuzzy subset inference method (FFSI method) is used here to realize the fuzzy inference process in fuzzy identification. As a result, there is the following FFSI fuzzy identification method for the most unfavorable thermal loop of air conditioning water system in the phase plane.

Let the measured values of the system real-time tracer direction vector angle β_i (kT) and the room temperature deviation e_i (kT) at the current moment be $(\beta^*$ and $e^*)$, and calculate the affiliation degrees $A_j(\beta^*)$ and $B_k(e^*)$ of β^* and e^* to A_j and B_k ($i, j = 1, 2, \dots, 7$), respectively, and their action fuzzy subsets as

$$\begin{aligned} \beta^* : A'_j, A'_j(\beta^*) > 0 \ \& \ A'_{j+1}, A'_{j+1}(\beta^*) > 0 \\ e^* : B'_k, B'_k(e^*) > 0 \ \& \ B'_{k+1}, B'_{k+1}(e^*) > 0 \end{aligned} \quad (4)$$

where $i, j = 1, 2, \dots, 7$. Find the action fuzzy control rules and the corresponding fuzzy amount of regulation C'_k from the action fuzzy subsets. Based on the fuzzy inference of the action fuzzy subsets, the truth value according to Equation (5) is

$$(A'_j \times B'_k)(\beta^*, e^*) = A'_j(\beta^*) \wedge B'_k(e^*) \quad (5)$$

According to Equation (5), the fuzzy quantity $C_{jk}^*(u)$ for the regulation quantity with the same canal tail is

$$C_{jk}^*(u) = \left\{ \left[(A'_j \times B'_k)(\beta^*, e^*) \right] \right\} C'_{jk}(u) \quad (6)$$

The fuzzy quantity $C^*(u)$ of the adjustment quantity is found.

$$C^*(u) = \bigvee_{k=1}^m C_k^*(u) \quad (7)$$

The center of gravity method is used to reverse-blur the fuzzy control quantity C^*

$$u^* = \frac{\sum_{k=1}^p C^*(u_k) \times u_k}{\sum_{k=1}^p C^*(u_k)} \quad (8)$$

The fuzzy identification method for the most unfavorable thermal loop, as illustrated in Figure 5, is presented herein. Firstly, the system's real-time tracing direction vector angle β_i (kT) and the current moment room temperature deviation e_i (kT) are selected as characteristic indices of the object under identification. Secondly, a triangular membership function is chosen as the affiliation function group for β_i (kT) and e_i (kT). Finally, based on the established affiliation function and employing fuzzy self-reasoning methodology, classification and identification of the object under consideration are performed. By comparing and analyzing the obtained degrees of unfavorability for each branch, it can be determined that the thermal loop with maximum value represents the most unfavorable condition at present time instant. Following this procedure enables preparation of an online phase plane fuzzy identification program specifically targeting such unfavorable thermal loops.

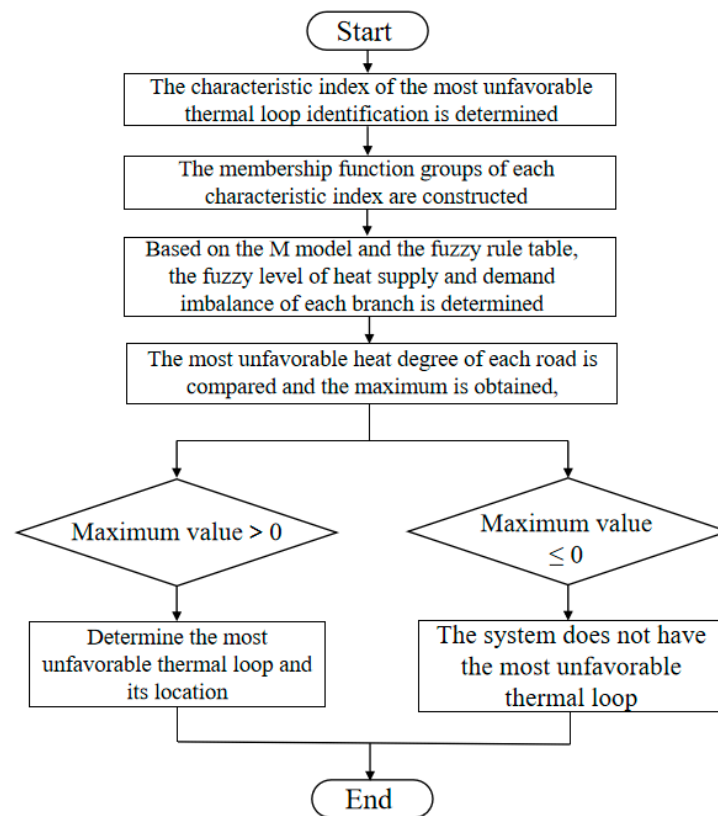


Figure 5. Flowchart of the most unfavorable thermal loop identification method.

3.2. Role of Pipe Network Models in the Control Process

During the regulation process of the pipe network, the impedance distribution is influenced by the end valve (electric two-way valve), while the impedance of main components in the machine room remains unchanged. Therefore, this study simplifies the pipe network system as follows: considering that there are no resistance adjustments or other components between the pump and manifold section, we treat this section as a simplified pipe segment b1 (with a flow rate equal to that of the entire system). The pipe network model is established accordingly, and nodes, trees, and branches within the system are divided and numbered. Based on this pipe network structure, both correlation matrix and basic loop matrix for this air conditioning water system are determined. By utilizing fundamental elements such as nodes and branches, we can divide the system model into six basic loops (each containing an end branch). The relationships among variables in these equations are complex and require iterative methods for solving. To simplify dimensionality of our model, we initially divide it into dendritic matrix A_t , continuous branch matrix A_l , flow vector tree G_t , and continuous branch flow matrix G_l , as illustrated in the equation below.

$$\begin{aligned} A &= [A_t, A_l] \\ G &= [G_t, G_l] \end{aligned} \quad (9)$$

Then, Equation (9) can be written as

$$AG = A G_t + A G_l = 0 \quad (10)$$

Since A_t is an invertible matrix, the above equation can be further transformed as

$$-A_t^{-1} A_t G_t + (-A_t^{-1} A_l G_l) = -A_t^{-1} Q \quad (11)$$

namely

$$G_t = A_t^{-1} Q - A_t^{-1} A_l G_l \quad (12)$$

The tree branch flow column vector can be represented by the node flow column vector and the continuous branch flow column vector. If G_1 is known, then G_t can be derived from Equation (12) to obtain the network flow matrix G , i.e., the objective of the solution is changed from the flow column vector G to the flow volume of each branch G_1 .

As we obtain

$$B_f(S|G|G - DH) = 0, \quad (13)$$

let the result of the $(k + 1)$ th iteration G^{k+1} be the solution of Equation (13), then

$$B_f\left(S \cdot \left|G^{k+1}\right| \cdot G^{k+1} - DH\right) = 0 \quad (14)$$

The results of the $(k + 1)$ th iteration G^{k+1} and G^k satisfy

$$G^{k+1} = G^k + \Delta G^{k+1} \quad (15)$$

where G^{k+1} is the difference vector between the $(k + 1)$ th iteration and the k th iteration of the connected branch flow.

Taking Equation (15) into Equation (14) and expanding it and omitting the quadratic term of G^{k+1} ,

$$B_f 2S \cdot \left|G^k\right| \cdot \Delta G^{k+1} = -B_f\left(S \cdot \left|G^k\right| \cdot G^k - DH\right) \quad (16)$$

also because

$$\Delta G^{k+1} = B_f^T \Delta G_1^{k+1} \quad (17)$$

Equation (17) is brought into Equation (16) as

$$B_f 2S \cdot \left|G^k\right| \cdot B_f^k \Delta G_1^{k+1} = -B_f\left(S \cdot \left|G^k\right| \cdot G^k - DH\right) \quad (18)$$

If

$$\begin{cases} M^k = B_f 2S \cdot \left|G^k\right| \cdot B_f^T \\ \Delta h^k = B_f(S \cdot \left|G^k\right| \cdot G^k - DH) \end{cases} \quad (19)$$

If Equation (19) is brought into Equation (18), then there is each time the amount of change in the flow of the connecting branch, satisfying

$$\Delta G_1^{k+1} = -M_k^{-1} \Delta h^k \quad (20)$$

When the second class of G^{k+1} has a parametric number less than the set accuracy, then the results of the two iterations before and after are the same, the requirements of this calculation process are satisfied, and the iteration process ends.

Based on the above solution process, the basic loop method is used to solve the flow rate and pressure drop of each pipe section in the system. As shown in Figure 6, the specific steps are described as follows:

1. For a given pipe network, the correlation matrix A and the basic loop matrix B_f , with impedance values S for each pipe segment, are created according to their structure;
2. Given an initial value of G_1^0 for even the tributary volume and a given iteration accuracy ε ;
3. The flow rate of the pipe network is obtained from the flow rate of the connected branch section, and the k th iteration of the connected branch flow column vector G_1^k is brought into the equation to obtain the flow rate vector G^k , which is brought into Equations (19) and (20) to obtain M^k and h^k , and then ΔG_1^k ;
4. The ΔG_1^{k+1} is brought into Equation (17) to obtain ΔG^{k+1} ;
5. Discriminate $\Delta G^{k+1} \leq \varepsilon$. If the condition is satisfied, stop the calculation and output the result $G^* = G^{k+1}$; otherwise, $k = k+1$ and repeat step (3).

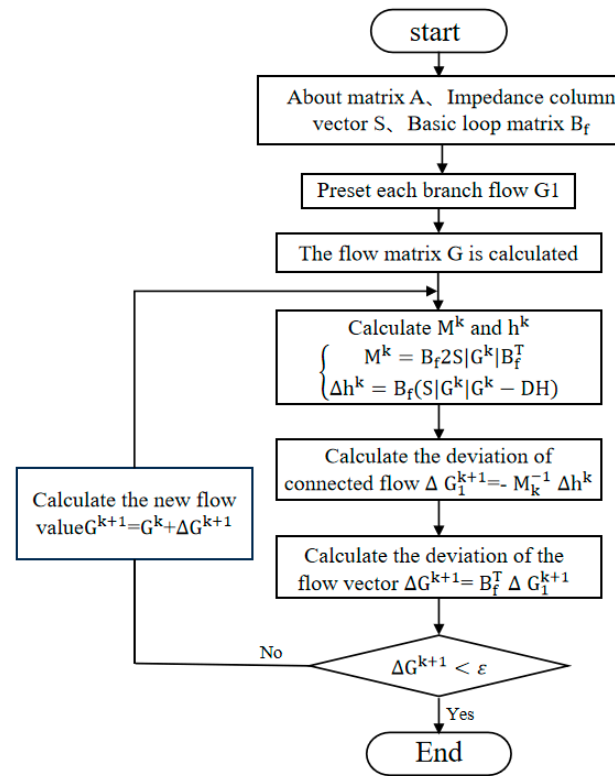


Figure 6. Flowchart of basic loop iterative calculation method.

3.3. Variable Pressure Differential Fuzzy Control Method Based on Identifying the Most Unfavorable Thermal Loop

In summary, it is only necessary to calculate $DP(kT)$ in real time according to the network model of online identification of the most unfavorable thermal loop, and then the setting value of the variable pressure difference can be realized. The algorithmic flow of the variable pressure differential fuzzy control method for chilled water systems based on identifying the most unfavorable thermal loop (VPDFC-IMUTL), as shown in Figure 7, is as follows.

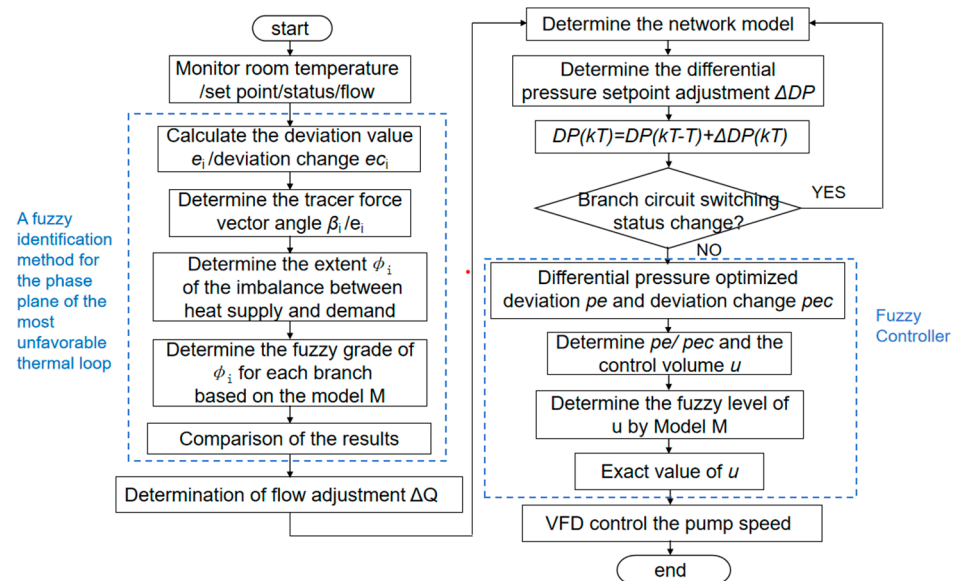


Figure 7. Flowchart of pressure differential adjustment algorithm in control cycle based on pipe network model.

Step 1: Online monitoring of air conditioning water system is established with indoor environment parameters including room temperature in each room and its setting value in the end controller, opening/closing state of each end branch electric switch valve, and pressure difference in each branch.

Step 2: Online identification of the most adverse thermal loop to the water system is achieved by calculating deviation e_i and deviation change value ec_i according to room temperature data. Real-time tracer direction vector angle β_i is determined in phase planar graph composed of $e-ec$, theoretical domain for β_i , e_i and imbalance degree $\Phi_i(\tau)$ is established. Fuzzy level $\Phi_i(\tau)$ is determined using Mamdani model with action fuzzy subset inference method (FFSI) and fuzzy rules. Results from all branches are obtained to ensure position of most unfavorable thermal loop and imbalance degree $\Phi_i(\tau)$.

Step 3: Online identification of key parameters of the most unfavorable thermal loop pipe network model is realized. As the end valves are regulated in real time during the system operation, when a branch valve is closed, the branch does not participate in the iterative cycle. Therefore, this method needs to monitor the opening and closing states of each valve in real time to adjust the structure of matrices A and B_f .

Step 4: Determine the pressure difference setting between the pump inlet and outlet, which includes

1. Obtaining the flow adjustment Q of the branch based on the aforementioned identification results of the most unfavorable thermal loop;
2. Calculating $\Delta DP(kT)$, the adjustment of the pump's inlet and outlet pressure difference set value using matrices A and B_f , and variations in flow for the most unfavorable thermal loop through basic loop method;
3. Obtaining re-normalized results of pressure difference set point using formula $DP(kT) = DP(kT - T) + \Delta DP(kT)$.

Step 5: Implement fuzzy control of pump frequency conversion FFSI method, including

1. Determining discourse domain and fuzzy level for deviation pe , deviation change value pec , and pump frequency u ;
2. Determining fuzzy level for u using M model and fuzzy control rule table;
3. De-fuzzifying through gravity center method to obtain precise value for pump frequency regulation u , enabling control over pump speed via VFD to achieve energy-saving control.

4. Case Study and Results Analysis

4.1. Variable Flow Air Conditioning System Test Bench

The air-conditioned room of the test bench comprises an equipment room, monitoring room, hall, and office, as depicted in Figure 8. The design load of the air conditioning in each room encompasses the cooling load of the envelope structure, internal heat sources, fresh air, and wet loads. Fan coils are positioned between these components. The office area is equipped with three fan coils; VAV air conditioning system has been implemented in the hall office area, hence only one fan coil is installed in the hall corridor; and the monitoring room is furnished with one fan coil. Each room's fan coils are numbered from 1# to 6#, with 1# located in the equipment room, 2#~4# situated in the office, 5# placed in the hall, and 6# positioned in the monitoring room.

Additionally, the schematic diagram in Figure 9 illustrates the variable flow air conditioning system plan for the test bench, comprising two components: the water system and the air system, where E represents the evaporator of a water source heat pump unit, and C represents its condenser. CHP1 and CHP2 denote circulating pumps within chilled water systems. CP1 and CP2 function as cooling water pumps; FCU1~6 represent individual end branches of each respective fan coil. AHU signifies an air conditioning unit while FHU stands for a fresh air unit. The main equipment, such as the chiller and the circulating water pumps in the machine room, is shown in Figure 10.

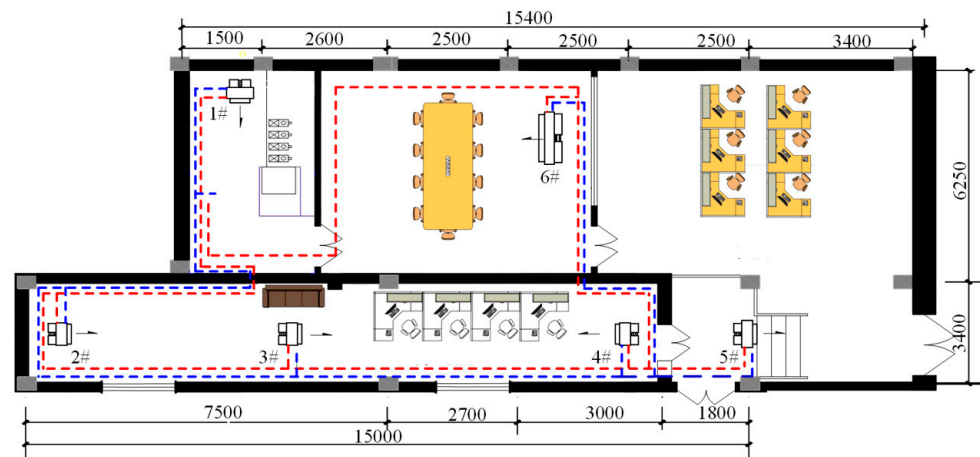


Figure 8. Plan of variable flow central air conditioning system and main equipment.

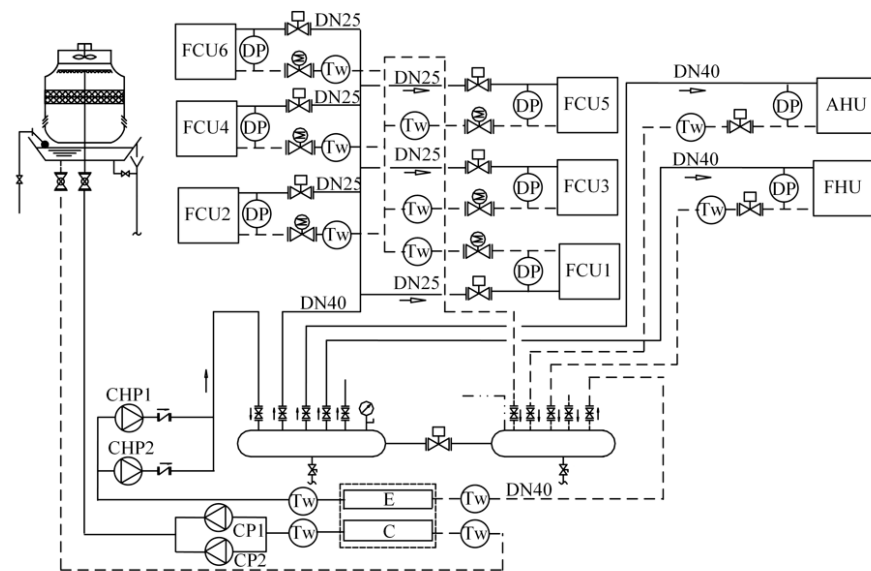


Figure 9. The water system schematic diagram of variable flow air conditioning.



Figure 10. Real picture of the machine room of variable flow air conditioning water system.

The main monitoring and control equipment of the test bench includes an intelligent temperature controller, a water temperature sensor, a pressure difference sensor, a temperature and humidity sensor for wet air, an ultrasonic flow meter, an electric continuous regulating valve, a frequency converter, an I/O module, PLC, and touch screen. In terms of communication and controller selection, the S7-1200CPU module body integrates one Ethernet interface and one RS485 interface with the option to extend the CM01 signal board. All CPU modules are equipped with standard Ethernet interfaces that support Siemens S7 protocol and TCP/IP protocol for various terminal connections. The S7-1200CPU module supports protocols such as Modbus-RTU, PPI, USS, free port communication, etc., which is utilized in this test system for data transmission. The WinCC server used with PLC enables man-machine interaction functions as well as database saving and exporting capabilities. Measurement and control points in the system are classified according to the main components of air conditioning; after determining the number of measurement and control points required, I/O expansion modules are selected to form link devices. For example, at the end of the fan coil branch measuring point, water supply/return pressure difference, continuous regulating valve position, two-way valve state, and return water temperature (3AI, 1DI) are included, while control point includes continuous regulating valve opening state of two-way valve (1AO, 1DO). Therefore, FCU linker includes AI module, AO module, DI module, and DO module.

4.2. Test Conditions

The end branch air conditioning rooms involved in the test include the equipment room, the monitoring room, the hall corridor, and the office, and the room temperature setting value of each room is set to 25 °C. The test was conducted on three adjacent days with similar meteorological conditions.

In order to quantitatively analyze the control and energy-saving effect of the proposed VPDFC-IMUTL for air conditioning water systems, three adjacent days with similar meteorological conditions were selected for the same length of time for the test, and the results of the application of the VPDFC-IMUTL method and the commonly used regulation results of the variable flow system were compared. The meteorological conditions from the 25th to 27th July are shown in Figure 8. During the test phase from 8:00 to 17:30, the ambient temperature and humidity did not differ much, the maximum daytime temperatures for the three days were 35.1 °C, 36.0 °C, and 36.0 °C, and the minimum temperatures were 31.8 °C, 31.8 °C, and 31.1 °C. The humidity ranges were 48.0% to 73.9%, 56.7% to 78%, and 48.2% to 73.7%, which can be regarded as the same meteorological conditions for comparative tests. The variable differential pressure fuzzy control method of the water system based on the identification of the most unfavorable thermal loop was applied on 25 July, the linear adjustment algorithm was applied on 26 July and the slope K was taken to be 0.5, and the linear adjustment algorithm was applied on 27 July and the slope K was taken to be 0.1. The fuzzy control method of the water system with variable differential pressure was applied to the water system based on the identification of the most unfavorable thermal loop.

4.3. Tests

In order to quantitatively analyze the actual regulation effect and energy consumption of the variable differential pressure fuzzy control method of water system based on the identification of the most unfavorable thermal loop in summer, experimental research was carried out by applying the variable differential pressure fuzzy control method of water system based on the identification of the most unfavorable thermal loop and the linear regulation method on 25th, 26th, and 27th of July from 8:00 to 17:00, respectively. In order to compare and analyze the regulation effect of the three algorithms on the end of the system, the trend of fan stall and water valve control and the trend of room temperature were analyzed in the case of 2# branch.

1. Control performance test results of variable differential pressure fuzzy control method for water system

As shown in Figure 9, in the regulation process (9:00~17:00), the room temperature and the set value of the time deviation were not large, the average value of room temperature in the test phase was 25.3 °C (the set value of 25 °C) with the maximum value of 25.9 °C and the minimum value of 24.7 °C. The results show that the supply of energy at the end of the supply is sufficient, and the effect of the room temperature control meets the user's needs. As shown in Figure 10, valve closing time is 139 min, and opening time is 402 min.

As shown in Figure 11, in the July 25th test regulation process, the pump speed regulation is relatively smooth, less pump speed surge conditions, by the influence of the environment. In the 8:00~9:00 and 13:30~15:00 processes, the pump is in 100% or 95% of the speed above the operation of the pump, and other times it is in a lower speed.

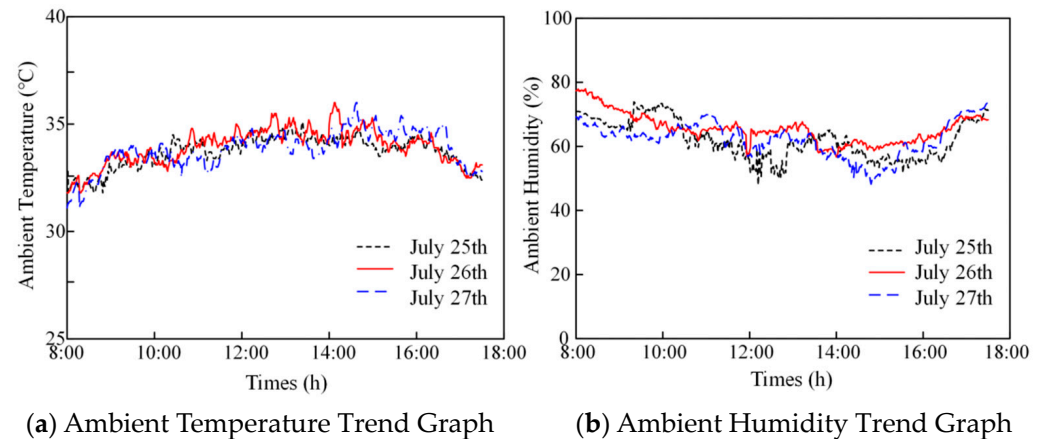


Figure 11. Trend chart of meteorological conditions.

2. Pump inlet and outlet pressure difference set value linear rectification method control performance test results

When $K = 0.5$, during the test regulation (9:00~17:00), the room temperature control effect is shown in Figure 12. The room temperature does not deviate much from the set value, and the average room temperature is 25.2 °C (the set value is 25 °C), the maximum value is 26.5 °C, and the minimum value is 24.4 °C, which indicates that the supply of energy at the end basically meets the demand of the branch circuit, the control amplitude of the room temperature is large, and the temperature of the room will be short-lived, deviating from the room temperature setting value. The regulation process of the valve and fan is shown in Figure 13. According to statistics, the valve closes for 95 min and opens for 356 min. In the regulation process, the fan gear from a high-grade to low-grade situation is more common, which is not conducive to meeting the user's requirements for comfort.

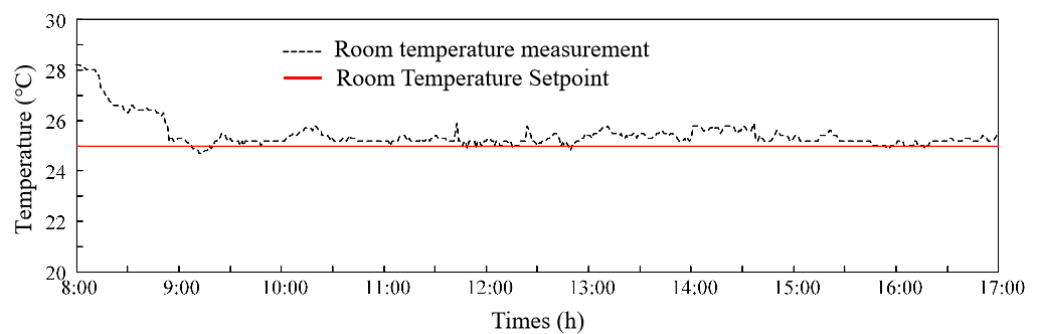


Figure 12. Effect of room temperature control on 25 July.

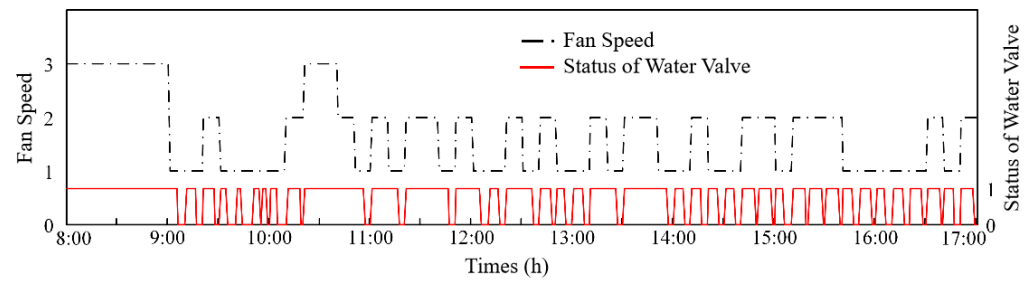


Figure 13. The water valve fan control on 25 July.

As can be seen from Figure 14 in the pump in the regulation process, there are many times that the process suddenly speeds up or slows down, which shows that the fixed regulation period for the algorithm is unreasonable. The main reason for this is that due to the variable differential pressure regulation process slope K value being too large, the pump imports and exports of the differential pressure set value changes too much, resulting in a frequent overshooting phenomenon of the system and, therefore, the end of the energy supply amount of excessive phenomena.

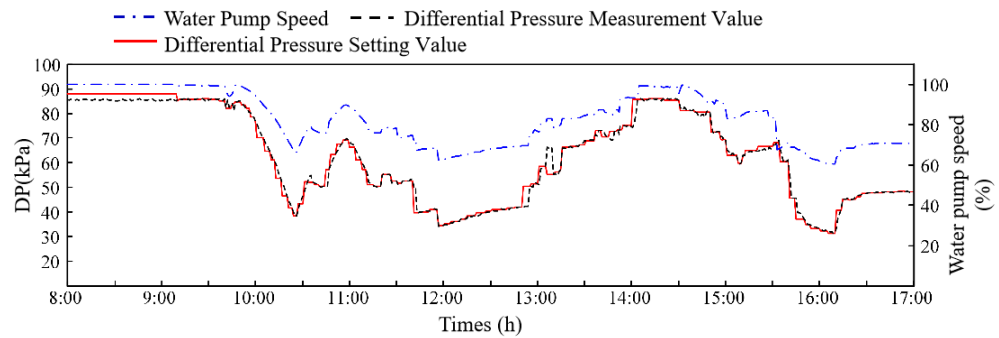


Figure 14. The trend chart of pressure difference before and after the system pump on 25 July.

The linear adjustment algorithm ($K = 0.5$) when the value of K is small is shown in Figure 15 in the test regulation process (8:00~17:00). The room temperature and the set point time deviation are not large, the average value of the room temperature is $25.2\text{ }^{\circ}\text{C}$ (set point $25\text{ }^{\circ}\text{C}$), the maximum value is $26.5\text{ }^{\circ}\text{C}$, and the minimum value is $24.4\text{ }^{\circ}\text{C}$. This indicates that the end energy supply adequately meets the branch's demand, but the room temperature control range is too wide, leading to brief deviations from the set value. The adjustment process of the valve and fan is illustrated in Figure 16. Statistical data shows that the valve remains closed for 95 minutes and open for 356 minutes. During regulation, it is common for the fan speed to be adjusted from high to low, which does not effectively meet user comfort requirements.

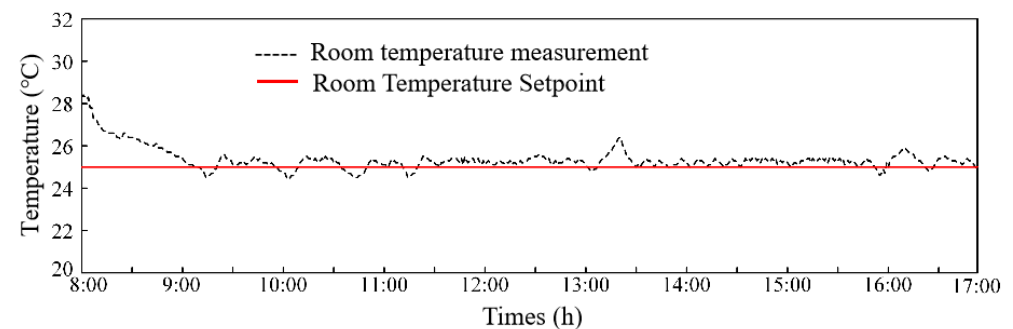


Figure 15. Effect of room temperature control on 26 July.

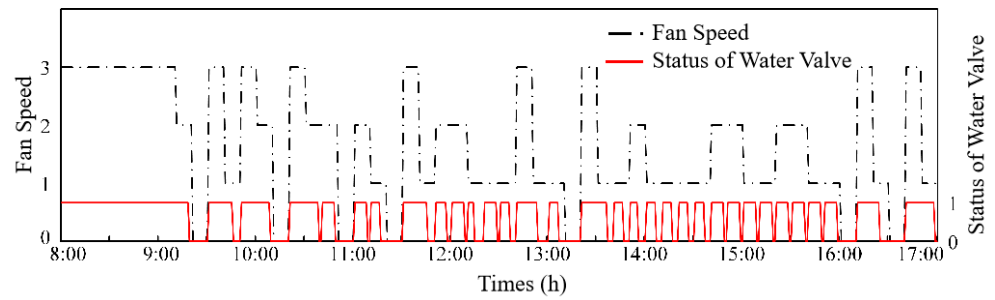


Figure 16. Water valve and fan speed control trend chart dated on 26 July.

It is evident from Figure 17 that the pump speed experiences frequent fluctuations during the regulation process, indicating that the fixed regulation period is not suitable for the algorithm. This is primarily due to an excessively large slope K value in the variable pressure difference regulation process, leading to significant changes in the pressure difference setting values at the inlet and outlet of the pump and resulting in frequent system overshoots, ultimately causing an excess of energy supply.

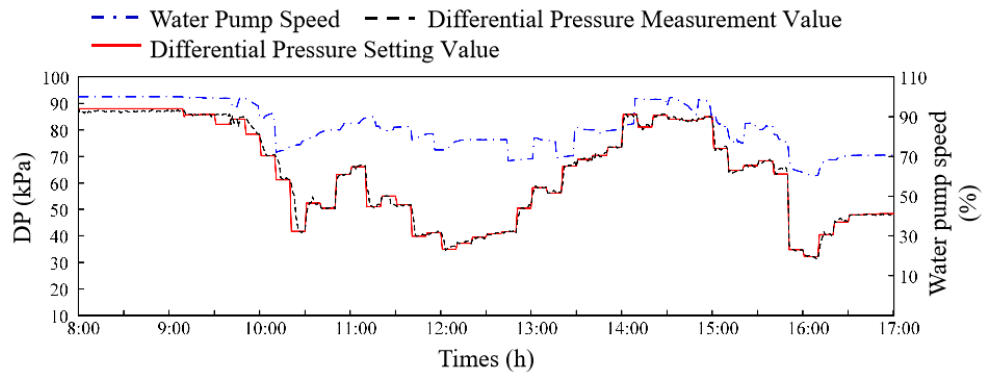


Figure 17. The trend chart of pressure difference before and after the system pump on 26 July.

The linear adjustment algorithm ($K = 0.1$) when the value of K is small is shown in Figure 18 in the test regulation process (8:00~17:00). The room temperature and the set point time deviation are not large, the average value of the room temperature is $25.4\text{ }^{\circ}\text{C}$ (set point $25\text{ }^{\circ}\text{C}$), the maximum value is $26.1\text{ }^{\circ}\text{C}$, and the minimum value is $24.5\text{ }^{\circ}\text{C}$, which indicate that the end of the energy supply amount basically meets the needs of each branch circuit. However, the room temperature is higher than $25\text{ }^{\circ}\text{C}$ for a longer period of time, which indicates that when there is insufficient supply, the system is slow to adjust, the room temperature for a longer period of time briefly deviates from the room temperature set value of the situation. As shown in Figure 19, the valve closing time is 62 min and the opening time is 389 min, during the regulation process; the fan gear is running in high and medium gears for a longer period of time; and the comfort at the end is poor.

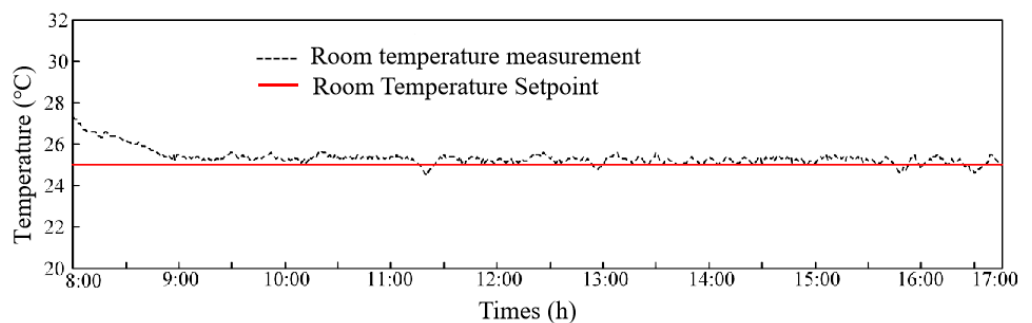


Figure 18. Trend chart of room temperature and set values on 27 July.

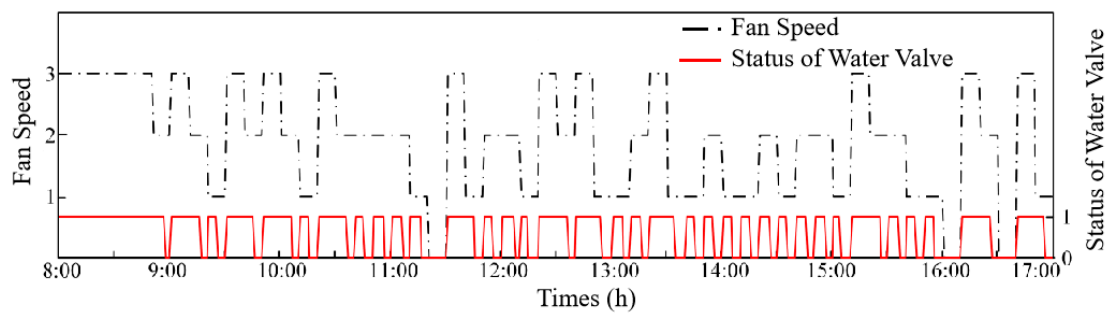


Figure 19. Water valve and fan gear control trend chart on 27 July.

As shown in Figure 20, during the control process, if the set value of the pump repeatedly increases or decreases for three consecutive times or more, it indicates that the adjustment amount of the set value in the algorithm is insufficient, making it difficult to meet the system's requirement for rapid elimination of the most unfavorable thermal loop.

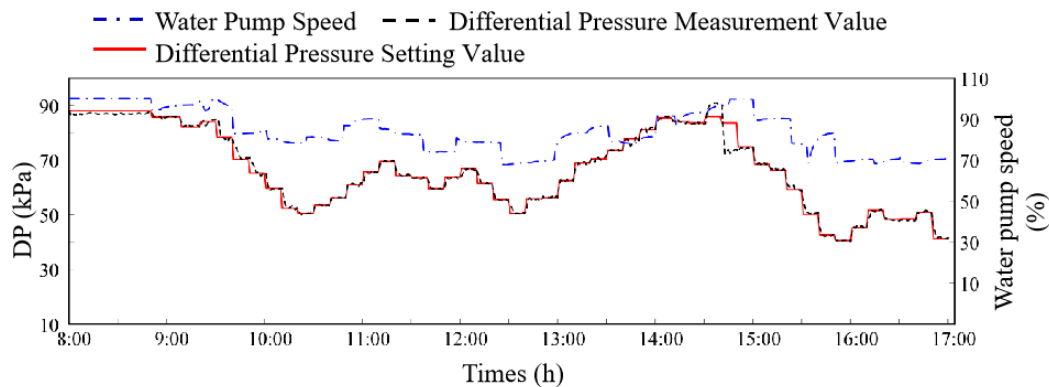


Figure 20. The trend chart of pressure difference before and after the system pump on 27 July.

4.4. Results Analysis

In order to analyze the impact of three different regulation methods on the end control and energy-saving effect of a variable flow air conditioning water system, various parameters were measured from 25 July to 27 July. The data collected include the energy consumption of water pumps, opening time of end valves, fan stall duration, and power consumption of water pumps. Detailed results are presented in Table 3. During testing, the total power consumption of the end fan was recorded as 1.13 kWh, 1.2 kWh, and 1.3 kWh, respectively, while that of the water pump was measured as 2.07 kWh, 2.21 kWh, and 2.05 kWh, respectively. Under normal operating conditions at industrial frequency levels, it is observed that one day's operation requires an energy consumption of approximately 3.33 kWh for fan coils and around 5.50 kWh for water pumps.

By applying a variable differential pressure fuzzy control method based on identifying unfavorable thermal loops within the water system, significant energy saving can be achieved compared to industrial frequency conditions—specifically up to a remarkable reduction rate of about 41.8%. Furthermore, when comparing with linear adjustment algorithms alone for controlling the water system based on identification of least favorable thermal loops within it, energy saving ranging from approximately 4.7% to about 6.5% can be obtained.

Considering the varying degree of the most unfavorable thermal loop at the system's end, the adjustment requirement for system energy differs. To address this, a variable differential pressure fuzzy control method is proposed for water systems based on identification of the most unfavorable thermal loop. This approach not only focuses on meeting energy demands at the end but also takes into account the role of pipeline networks in flow rate distribution. Consequently, it reduces pump adjustment time and minimizes flow

distribution impact caused by end valve regulation, thereby achieving energy-saving goals in pump operation.

Table 3. Summary table of system operation energy consumption statistics.

Test Methods	Energy Consumption Statistics (kWh)		Energy Saving (%)
	Fan Coil Electricity Consumption	Electricity Consumption of Water Pumps	
System frequency operation (pump speed 50 Hz, fan in high gear)	3.33	5.49	-
VPDFC-IMUTL	1.13	2.07	41.8
Linear adjustment algorithm $K = 0.5$	1.20	2.21	38.0
Linear adjustment algorithm $K = 0.1$	1.30	2.05	39.1

5. Conclusions and Future Works

The present paper proposes an online identification method for key parameters of the air conditioning water system pipe network model, as well as a fuzzy identification method for the phase plane of the most unfavorable thermal loop. Furthermore, it introduces a fuzzy control method that utilizes action fuzzy subset inference and a variable differential pressure fuzzy control approach based on identifying the most unfavorable thermal loop. Additionally, computer-networked monitoring and control technology is developed, and experimental research is conducted using a test bench of a variable flow air conditioning water system.

1. This approach enables online identification of air conditioning water systems to serve as a suitable control reference loop for achieving energy-saving control of pump frequency conversion differential pressure set values.
2. On the phase plane controlled by room temperature, any state point appearing at quadrant I of an end branch may represent the most unfavorable thermal loop. The likelihood of an end branch being identified as the most unfavorable thermal loop is closely associated with the angle of its real-time tracer vector on this phase plane. A larger angle at (0° , 180°) indicates a higher probability for that user branch to become identified as having a critical thermal loop.
3. Compared with traditional linear variable differential pressure set point control algorithms, this method achieves remarkable energy saving ranging from 4.7% to 6.5%.

In future studies, we will further investigate this approach in order to subsequently explore energy-efficient control strategies for the entire central air conditioning system. This paper still has the following work that needs to be studied.

1. The promotion and implementation of the concept, definition, determination, and online identification method of the most unfavorable thermal loop based on heat supply balance in HVAC air systems, heating systems, and central heating systems are crucial.
2. The engineering application of a variable pressure differential fuzzy control method for water system based on the identification of the most unfavorable thermal loop in energy conservation regulation of different water systems still requires further research. The energy consumption in large public construction operation from variable flow air conditioning water systems is substantial with considerable potential for energy saving. Therefore, applying this method to practical projects can achieve significant energy saving. The focus should be on exploring how to promote and apply it in various forms of water systems.
3. This algorithm utilizes the Siemens S7-1200 series PLC, which imposes higher demands on the controller compared to traditional linear algorithms. Additionally, the

increased sensor component at the end results in significantly higher costs, a factor that should be considered during the promotion process.

Author Contributions: Conceptualization, T.C.; methodology, T.C.; experiment and result analysis, T.C. and Y.H.; writing—original draft preparation, Y.H.; writing—review and editing, T.C. All authors have read and agreed to the published version of the manuscript.

Funding: This research received no external funding.

Data Availability Statement: No new data were created.

Acknowledgments: This work was supported by the Plan of Introduction and Cultivation for Young Innovative Talents in Colleges and Universities of Shandong Province.

Conflicts of Interest: The authors declare no conflicts of interest.

References

1. Fathollahzadeh, M.H.; Tabares-Velasco, P.C. Integrated framework for optimization of air- and water-side HVAC systems to minimize electric utility cost of existing commercial districts. *Energy Build.* **2022**, *273*, 112328. [[CrossRef](#)]
2. Gidwani, B.N. Optimization of Chilled Water Systems. *Energy Eng. J. Assoc. Energy Eng.* **1984**, *84*.
3. Wang, S.; Burnett, J. Online adaptive control for optimizing variable-speed pumps of indirect water-cooled chilling systems. *Appl. Therm. Eng. Des. Process. Equip. Econ.* **2001**, *21*, 1083–1103. [[CrossRef](#)]
4. Mba, L.; Meukam, P.; Kemajou, A. Application of artificial neural network for predicting hourly indoor air temperature and relative humidity in modern building in humid region. *Energy Build.* **2016**, *121*, 32–42. [[CrossRef](#)]
5. Wang, N.; Zhang, J.; Xia, X. Energy consumption of air conditioners at different temperature set points. *Energy Build.* **2013**, *65*, 412–418. [[CrossRef](#)]
6. Ma, Z.; Wang, S. Energy efficient control of variable speed pumps in complex building central air-conditioning systems. *Energy Build.* **2009**, *41*, 197–205. [[CrossRef](#)]
7. Gao, D.C.; Wang, S.; Sun, Y. A fault-tolerant and energy efficient control strategy for primary–secondary chilled water systems in buildings. *Energy Build.* **2011**, *43*, 3646–3656. [[CrossRef](#)]
8. Takagi, T.; Sugeno, M. Fuzzy identification of systems and its applications to modeling and control. *IEEE Trans. Syst. Man Cybern.* **1985**, *SMC-15*, 116–132. [[CrossRef](#)]
9. Fisher, B.J.M.D. Pump Differential Pressure Setpoint Reset Based on Chilled Water Valve Position. *ASHRAE Trans.* **2003**, *2003*, 371–377.
10. Liu, X.; Liu, J.; Lu, Z.; Xing, K.; Mai, Y. Diversity of energy-saving control strategy for a parallel chilled water pump based on variable differential pressure control in an air-conditioning system. *Energy* **2015**, *88*, 718–733.
11. Jiang, X.; Xu, Y.; Fang, Y. Energy-saving control strategy for chilled water systems of primary-secondary-tertiary pump. *J. Fujian Univ. Technol.* **2014**.
12. Zhao, T.; Ma, L.; Zhang, J. An optimal differential pressure reset strategy based on the most unfavorable thermodynamic loop on-line identification for a variable water flow air conditioning system. *Energy Build.* **2016**, *110*, 257–268.
13. Suamir, I.N.; Ardita, I.N.; Santanu, G. Experimental and numerical optimization on chilled water configuration for improving temperature performance and economic viability of a centralized chiller plant. In *Conference Series, Proceedings of the International Conference on Applied Science and Technology, Bali, Indonesia, 24–25 October 2019*; IOP Publishing Ltd.: Bristol, UK, 2020.
14. Cross, H. Analysis of flow in networks of conduits or conductors. *Univ. Ill. Bull.* **1936**, *286*, 42–47.
15. Yu, J.; Liu, Q.; Zhao, A.; Chen, S.; Gao, Z.; Wang, F.; Zhang, R. A distributed optimization algorithm for the dynamic hydraulic balance of chilled water pipe network in air-conditioning system. *Energy* **2021**, *223*, 120059. [[CrossRef](#)]
16. Morales, E.L.; Aguilar, J.; Garcés-Jimenez, A.; Gutierrez De Mesa, J.A.; Gomez-Pulido, J.M. Advanced fuzzy-logic-based context-driven control for HVAC management systems in buildings. *IEEE Access* **2020**, *8*, 1. [[CrossRef](#)]
17. Cai, X.; Jin, Z.; Li, H.; Kümpel, A.; Müller, D. Automated PLC Code Generation for the Implementation of Mode-Based Control Algorithms in Buildings. *Buildings* **2024**, *14*, 73. [[CrossRef](#)]

Disclaimer/Publisher’s Note: The statements, opinions and data contained in all publications are solely those of the individual author(s) and contributor(s) and not of MDPI and/or the editor(s). MDPI and/or the editor(s) disclaim responsibility for any injury to people or property resulting from any ideas, methods, instructions or products referred to in the content.